A&A manuscript no.
(will be inserted by hand later)

Your thesaurus codes are:
(08.14.2;02.01.2;08.09.2 IP Peg)

ASTRONOMY
AND
ASTROPHYSICS
9.1.1999

Double Dataset Eclipse Mapping of IP Peg

Andreas Bobinger[1], Heinz Barwig[1], Hauke Fiedler[1], Karl–Heinz Mantel[1], Damir Šimić[2] and Sebastian Wolf[3]

[1] Universitäts-Sternwarte, Scheinerstr. 1, D–81679 München, Germany
[2] Max–Planck–Institut für extraterrestrische Physik, Giessenbachstr. 1, D–85740 Garching, Germany
[3] ESO - European Southern Observatory, Karl–Schwarzschild–Str. 2, D–85748 Garching, Germany

Received date; accepted date

Abstract. The classical Eclipse Mapping Method, developed by Horne (1985), allows to get a deeper insight into the spatial structure of accretion disks. Reconstructing a two-dimensional intensity distribution from an one-dimensional dataset of the light curve, the method is not artifact–free and the result depends on the used default image. Using simultaneously recorded trailed spectra and photometry as a double dataset, we are able to reconstruct accretion disks nearly without artifacts. It is possible to resolve structures in the accretion disk with very high clarity and reliability. The Double Dataset Eclipse Mapping is applied to the dataset of the cataclysmic variable IP Peg. The reconstructions show an asymmetric disk with a second spot, opposite to the hot-spot of the impact region of the gas-stream in the Doppler-maps which can be now unequivocally assigned in the eclipse-maps to emission in the adjacence of the hot-spot, to the central part of the accretion disk and a region opposite to the hot-spot at the outer part of the disk. The possible origin and nature of these features are discussed.

Key words: stars: cataclysmic variables – accretion disks – individual: IP Peg

1. Introduction

Cataclysmic variable stars (CVs) are close binary systems, containing a late main-sequence star and a white dwarf primary star. Material is transferred from the Roche-lobe filling secondary star towards the primary star by means of a gas stream. The angular momentum of this stream is too high to fall directly onto the white dwarf. Instead an accretion disk is formed, where the action of viscosity allows the material to slowly spiral inward towards the primary star. A hot spot is formed on the disk at the stream impact region. Most of these binary systems undergo outburst states which vary in duration and brightness. Dwarf novae are a subgroup of CVs showing quasi-periodic outbursts at intervals of tens to hundreds of days in which they brighten by several magnitudes.

Send offprint requests to: A. Bobinger

Two different methods have been developed to investigate CVs, namely Eclipse Mapping and Doppler Tomography. The Eclipse Mapping Method allows to get a spatial reconstruction of the intensity distribution of accretion disks from light curves (Horne 1985, Horne 1991, Horne 1995, Horne & Cook 1985, Horne & Marsh 1986, Baptista & Steiner 1993, Rutten et al. 1992a, Rutten et al. 1992b, Rutten & Dhillon 1994, Bobinger et al. 1997). Doppler Tomography (Marsh & Horne 1988, Horne 1991) reconstructs the intensity distribution of the accretion disk in velocity-coordinates. Doppler maps are computed from trailed spectra and are able to resolve and separate the intensity distribution of the individual components in a semi-detached binary system, like secondary, hot spot and disk. Both methods are now established as standard applications to investigate the accretion dynamics in disks of cataclysmic variables.

In this paper we present a re-analysis of our previous work (Wolf et al. 1998) by applying an extension of the classical Eclipse Mapping Method, the Double Dataset Eclipse Mapping, to the deeply eclipsing dwarf nowa IP Peg (discovered by Lipovetskij & Stepanyan, 1981). In Sect. 2 we describe the evolution of the improved method and the related tests to model data. Section 3 deals with the application of the method to real data, whereas Sect. 4 gives a discussion and an outlook.

2. The Method and Tests

2.1. Classical Single Dataset Eclipse Mapping and its Results

The classical Eclipse Mapping uses the maximum entropy fitting package MEMSYS (Skilling 1981, Skilling & Bryan 1984) to compute a maximum entropy reconstruction of an accretion disk, using an one-dimensional light curve as input dataset. In a cataclysmic variable with a sufficiently high inclination, the accretion disk and all related light sources like the hot spot, the white dwarf or any emitting structure in the disk undergo a periodical eclipse by the secondary star, creating an unambiguous feature in the light curve.

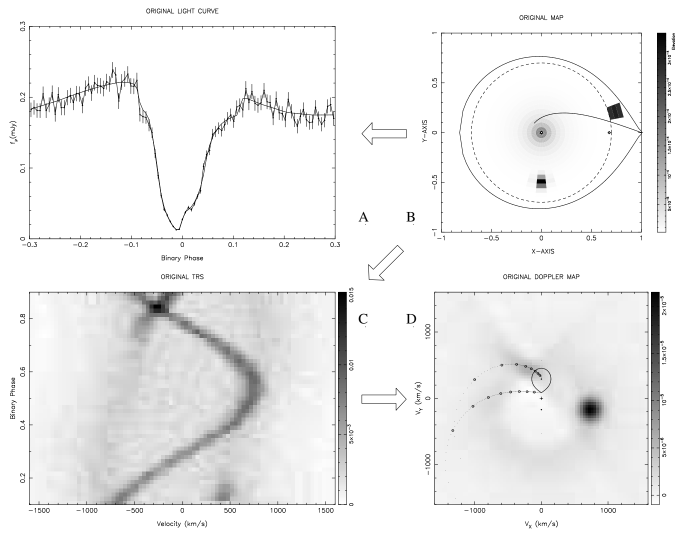

Fig. 1. Original test map: Panel A : light curve between phase -0.2 and +0.2. in arbitrary units. Panel B : Intensity distribution of the test map in position-coordinate representation. The dashed circle represents the outer disk radius. Pixels outside the dashed circle belong to the rim and are folded upward for plotting reasons. Also the Roche lobe and the gas stream trajectory are plotted. The unit is the distance between the white dwarf and the inner Lagrangian point. Panel C : Trailed spectra derived from the map in Panel B, assuming a Keplerian velocity field. Panel D : Doppler-map, reconstructed from the trailed spectra shown in panel C with a Fourier-filtered back-projection algorithm. A schematic overlay marks the Roche-lobe of the secondary as well as the ballistic trajectory which originates from the L_1 point. Additionally plotted is a second trajectory which represents the velocity of the disk along the path of the gas stream.

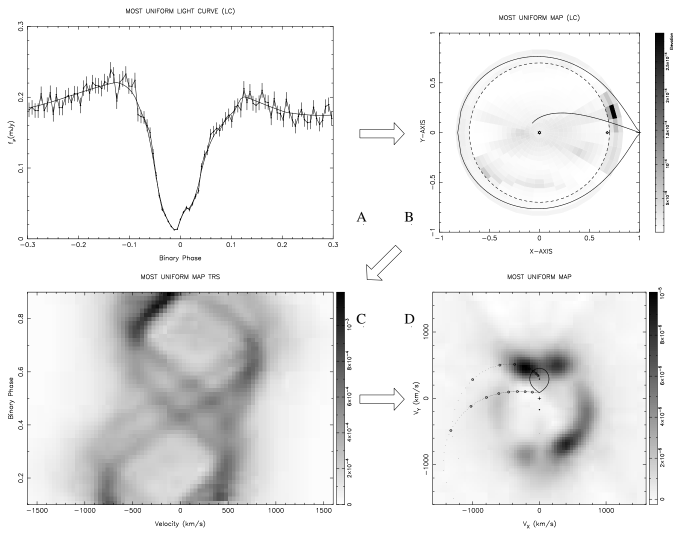

Fig. 2. Most Uniform Reconstruction of the original map, shown in Fig. 1, panel B, using the light curve as shown in Fig. 1 (panel A), as the only input dataset. Panel A in this plot shows the input data and the fit to the light curve (solid line). Panel B shows the reconstruction in space-coordinate representation. Panel C presents the trailed spectra, derived from the map in panel B under the assumption of a Keplerian velocity field. Panel D visualizes the corresponding Doppler-map in velocity-coordinates.

The Eclipse Mapping method reconstructs the intensity distribution of the accretion disk on a two-dimensional grid, in order to fit the observed data within a maximum allowed χ^2 deviation, called CAIM. MEMSYS is thereby varying the intensity of the pixel grid until the χ^2 of the model reaches CAIM. Then the pixel values are varied to maximize a defined image entropy, holding the constrained χ^2 = CAIM. The image entropy is maximized with respect to a default image. Three variations of default images are commonly established:

- Most Uniform Default Image:
  Each pixel of the default image has the average value of the total intensity of the actual image. The corresponding reconstruction is called ”Most Uniform Reconstruction.”
- Smoothest Default Image:
  The default image is a Gaussian smoothed version of the actual image. The corresponding reconstruction is called ”Smoothest Reconstruction.”
- Most Nearly Axisymmetric Default Image:
  The default image is also a Gaussian smoothed version of the actual image. But the Gaussian weight is low in radius and very high in azimuth. The corresponding reconstruction is called ”Most Nearly Axisymmetric Reconstruction.”

The default images are necessary because one dimension of information is missing. The light curve is one-dimensional and the reconstruction is two-dimensional. The maximum entropy solution is the solution with the lowest amount of bias, and therefore the most reliable one. The most uniform solution is *the* solution for the ”one-dimensional light curve”-problem. But because up to now an accretion disk was expected to be axisymmetric, the most nearly axisymmetric reconstruction is widely established. This way to reconstruct an accretion disk pushes the character of the default image into the solution. The solution is depending on the default image.

Beyond the classical method is not able to reconstruct anisotropic radiating light sources like the hot spot. The hot spot is situated at the outer rim of the disk, where the gas stream from the secondary hits the disk and radiates outward in the orbital plane. So there are orbital phases where the hot spot is seen by the observer face-on, and phases where the hot spot is hidden behind the disk. This produces a structure called the ”hump” in the light curve. Because of the flat grid used by the algorithm, this hump cannot be reconstructed. All pixels are assumed to radiate at each phase like Lambert radiators and have therefore the same radiation characteristics at each phase. To reconstruct such light sources like the hot spot, we changed the algorithm in some aspects. First, we introduced a disk opening angle and an outer rim, wrapped around the disk. This rim consists of three pixel rows, simulating the outer side of a torus. To match the rim and the outer regions of the disk more properly, we also changed the geometry of the grid from cartesian to polar coordinates. So we are able to get a more realistic reconstruction-surface and

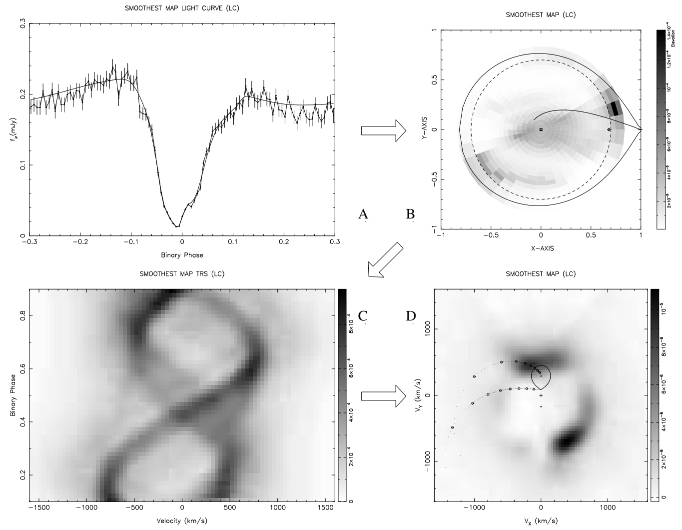

Fig. 3. Smoothest Reconstruction of the original map, shown in Fig. 1, panel B, using the light curve as shown in Fig. 1 (panel A), as the only input dataset. Panel A in this plot shows the input data and the fit to the light curve (solid line). Panel B shows the reconstruction in space-coordinate representation. Panel C presents the trailed spectra, derived from the map in panel B under the assumption of a Keplerian velocity field. Panel D visualizes the corresponding Doppler-map in velocity-coordinates.

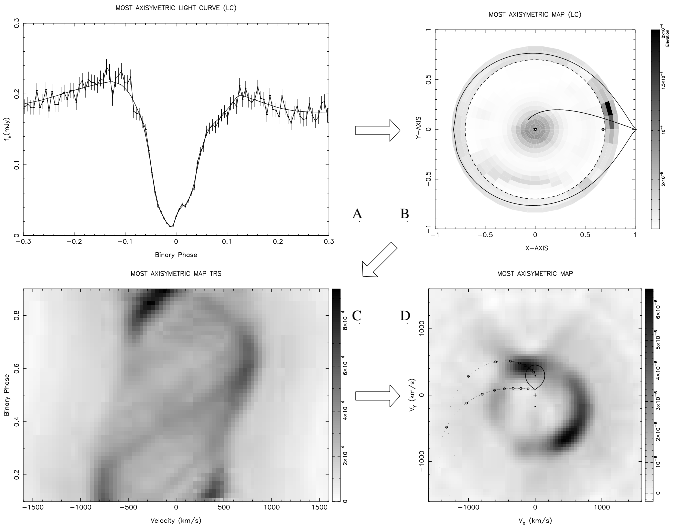

Fig. 4. Most Nearly Axisymmetric Reconstruction of the original map, shown in Fig. 1, panel B, using the light curve as shown in Fig. 1 (panel A), as the only input dataset. Panel A in this plot shows the input data and the fit to the light curve (solid line). Panel B shows the reconstruction in space-coordinate representation. Panel C presents the trailed spectra, derived from the map in panel B under the assumption of a Keplerian velocity field. Panel D visualizes the corresponding Doppler-map in velocity-coordinates.

the ability to reconstruct anisotropic light sources like the hot spot, by providing outward facing pixels with phase-depending radiation behavior. We also implemented the ability to tilt the rim-pixels in the impact region of the gas stream by a certain angle to simulate non radial radiation of the hot spot. The outward facing rim was first used by Bobinger et al. (1997), and later independently developed by Rutten (1998).

To visualize the dependence of the solution from the default image, we created a model accretion disk map. This map has increasing intensity towards the center and a hot spot at the rim near the impact region of the gas stream. To test the feasibility of the reconstruction algorithm to non-axisymmetric light sources we added a second spot onto the disk. From this artificial disk we calculated a light curve and added Gaussian noise to simulate real data. This light curve was then used as input data to the Eclipse Mapping algorithm to reconstruct the original map. From this map a trailed spectrum can be also calculated by assuming a certain velocity field. To do this, we assumed a Keplerian velocity field to transform the map from position-coordinate representation into a trailed spectrum. We also added Gaussian noise to the spectrum to simulate real data. Doppler Tomography now allows to calculate the intensity distribution of the original map in velocity-coordinates by using this trailed spectra as input data. Figure 1 shows in four sub-panels the artificially created map (panel B), the derived light curve (panel A), the trailed spectra (panel C) derived from the map (panel B) and finally the Doppler-map (panel D) calculated from the trailed spectra, assuming a Keplerian velocity field for the disk. The arrows between the panels clarify the data-flow. In Figs. 2, 3 and 4 the reconstructions using the light curve and different default image modes are presented. Figure 2 shows the Most Uniform, Fig. 3 the Smoothest and Fig. 4 the Most Nearly Axisymmetric Reconstructions. Especially the Most Uniform and the Smoothest Reconstruction show strong artifacts (panels B). The intensity of the disk center and the spot on the disk is distributed along the ingress- egress-arcs of the secondarys shadow. All this artifacts are producing features in the trailed spectra calculated from the maps (see panels C) and also in the Doppler maps (panels D).

2.2. *Double Dataset Eclipse Mapping*

The basic assumptions of Double Dataset Eclipse Mapping are very simple. Every structure in the map produces a signal in the trailed spectrum. Also every artifact does! By using trailed spectra and light curve as a double dataset, artifacts will be automatically suppressed. The signal in trailed spectra produced by artifacts in the reconstruction, has no counterpart in the observed trailed spectra. To deal with the double dataset, we had to split up our OPUS and TROPUS routines, which communicate between the user-problem and the main MEMSYS algorithm, into two parts. The light curve part acts as usual by simulating the eclipse of the disk by the secondary, the spectroscopic part transforms the actual image via the assumed Keplerian velocity field into trailed spectra. The only disadvantage of this method is, that it is constrained to emission line light curves and trailed spectra from emission lines. To test this, we used the light curve of the original map (Fig. 1 panel A) and the trailed spectrum

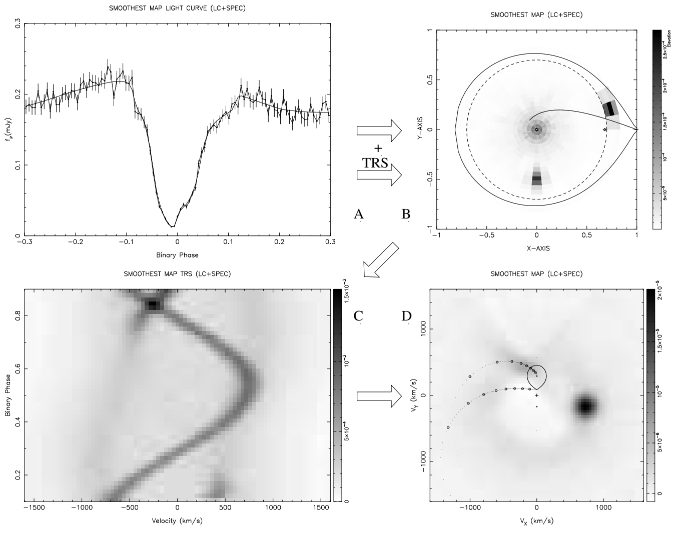

Fig. 5. Double Dataset Reconstruction of the original map, shown in Fig. 1, panel B, using the light curve and the trailed spectra shown in Fig. 1, panels A & C, as the input dataset. The Smoothest Default Image mode was used. Panel A in this plot shows the input data and the fit to the light curve (solid line). Panel B shows the reconstruction in space-coordinate representation. Panel C presents the trailed spectra, derived from the map in panel B under the assumption of a Keplerian velocity field. Panel D visualizes the corresponding Doppler-map in velocity-coordinates.

derived from the original map (Fig. 1 panel C) as input data. Figure 5 shows the reconstruction of the original map. Figure 5, panel C, shows the trailed spectrum, derived from the reconstructed map (panel B), assuming again a Keplerian velocity field. The smoothest default image mode was used for the reconstruction. These solution shows no artifacts and is nearly identical with the original.

3. Application to Real Data

3.1. The Dataset

During an observing campaign in August 06 – 09 1994 we performed simultaneous spectroscopy at the 3.5m and spectrophotometry at the 2.2m telescopes at the German-Spanish Astronomical Center, Calar Alto, Spain, to get data from the cataclysmic variable IP Peg during quiescence. From the trailed spectroscopic dataset we extracted the H_γ, H_β and H_α Balmer-lines. The spectrophotometric data were recorded with the MEKASPEK device of the Universitäts-Sternwarte Munich (Mantel 1993, Mantel & Barwig 1993) and enabled us to extract photometric light curves of the Balmerlines H_γ, H_β and H_α. Data acquisition and the reduction methods used are described and explained in detail in Wolf et al. (1998) and Šimić et al. (1998). We find it useful to present again the original trailed spectra and the corresponding original Doppler maps, together with the light curves in Fig 6. Details are given in the captions. The line-flux was separated from the continuum in the trailed spectra and the spectrophotometric data as follows: We cutted out the emission lines from the datasets and filled the gaps via spline interpolation to get the continuum. Then the line-spectrum was obtained by subtracting the continuum from the dataset. This approach was made to both, the spectroscopy and the spectrophotometry. To increase the signal-to-noise ratio of the data, we averaged the data of the second and third night. The first night was omitted because the eclipse was not totally recorded (see Wolf et al. 1998). The disadvantage of this method is, that noise, belonging to the continuum, is partially left in the line flux because of the splining. So the line light curves are more noisy than they really are. To reduce this, we smoothed the light curve with a narrow boxcar-filter operating in gliding mean mode.

3.2. The Results

We used the original trailed spectra presented in Fig. 6 and the H_γ, H_β and H_α emission line light curves as input dataset to reconstruct the accretion disk of IP Peg in this emission lines.

Trial reconstructions with different tilt-angels for the rim-pixels in the hot spot region, lead to a tilt-angle of $-60°$ outward, i.e. away from the secondary. Thereby the angle is measured between the direction radial outward from the primary and the normal vector of the rim-pixel. For this tilt-angle the maximum entropy was derived. Details are described in Wolf et al. 1998.

Figures 7, 8 and 9 show the results. Panels A show the smoothed light curves from the MEKASPEK dataset and the fit (solid line) to the data. In panels B the reconstructions are plotted, panels C present the trailed spectra derived from the reconstructions shown in panels B. In panels D the Doppler maps, derived from the trailed spectra in panels C, are presented. Comparison of the Doppler maps in panels D with the original Doppler maps in Fig. 6 show good global agreement. The main difference is the region of the hot spot and the secondary star. The hot spot in the original Doppler maps is more distorted than in the Doppler maps derived from the reconstructions. This can be explained by our assumptions made for the velocity field. To transform the maps into spectra we assumed an overall Keplerian disk. But in the region of the hot spot, where the velocities of the outer disk and the gas stream are mixing, the disk is probably not Keplerian. A recent work of Spruit & Rutten (1998) studies the emission properties of the hotspot of WZ Sge, which has a similar structure in the Doppler maps as IP Peg. The authors explain the different hot spot emissions with mixing postshock flows from the disk material and from the incomming stream.

The secondary star is not included in our reconstruction algorithm. Hence no feature of the secondary can be seen in the panels D in Fig. 7, 8 and 9, despite the presence of the secondary in the original Doppler maps in Fig. 6, i.e. in H_β and H_α. The secondary is too "cool" to produce any signature in H_γ. The contribution of the secondary in H_β is very weak and the distortion of the reconstruction is not detectable. In H_α the absence of a secondary-model in the reconstruction algorithm should lead to artifacts at the upper and lower part of

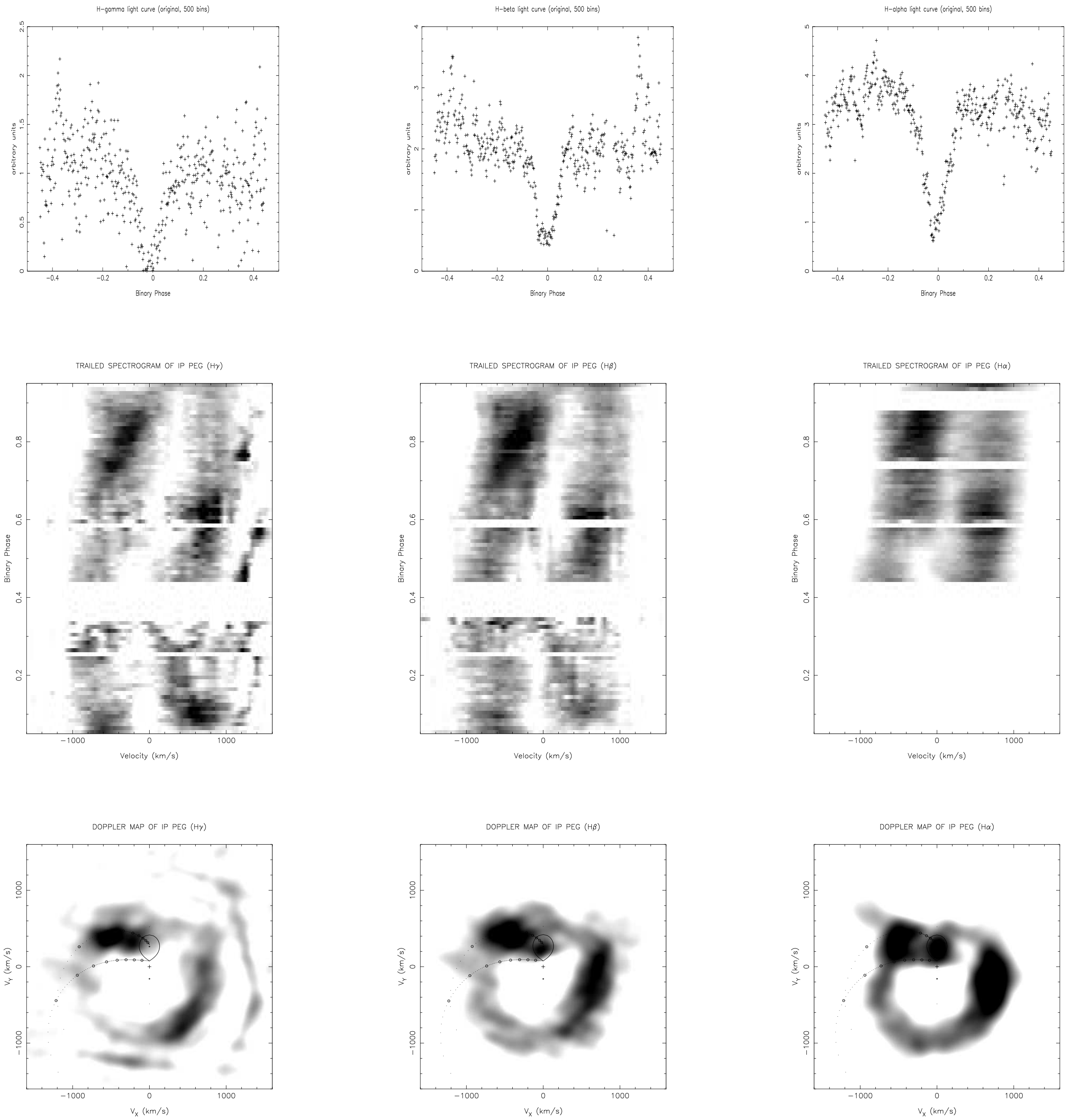

Fig. 6. Original dataset: Top row: From left to right, the original unfiltered line light curves are plotted. Middle row: From left to right, the original trailed spectra in H_γ, H_β and H_α are presented. The continuum under the emission lines was subtracted via spline interpolation. Not covered phase ranges are marked with empty white rows. Note, that we could only obtain 50% phase coverage of H_α due to technical difficulties. Bottom row: From left to right, the corresponding Doppler maps are shown in velocity space ($V_X\,;V_Y$). The maps were calculated from the above trailed spectra using the Fourier-filtered back-projection technique. A schematic overlay marks the Roche-lobe of the secondary as well as the ballistic trajectory which originates from the L_1 point. Additionally plotted is a second trajectory which represents the velocity of the disk along the path of the gas stream.

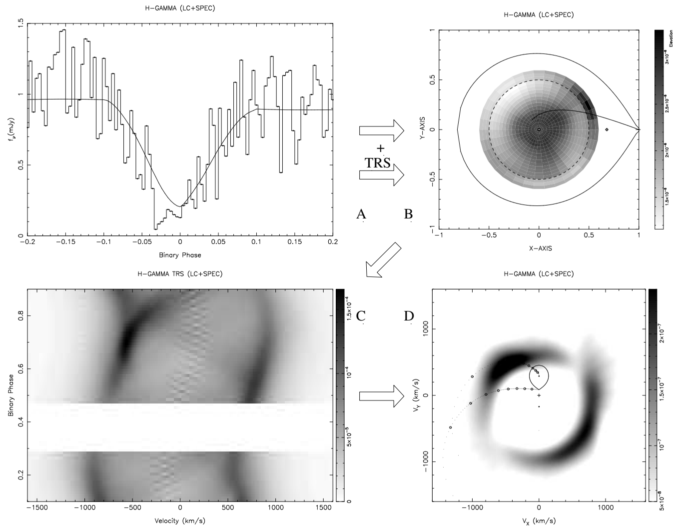

Fig. 7. Double dataset reconstruction in H_γ, using the light curve and the trailed spectra shown in Fig. 6 top left, as input dataset. Panel A in this plot shows the input data and the fit to the light curve (solid line). Panel B shows the reconstruction in position-coordinate representation. Panel C presents the trailed spectra, derived from the map in panel B under the assumption of a Keplerian velocity field. Panel D visualizes the corresponding Doppler-map in velocity-coordinates.

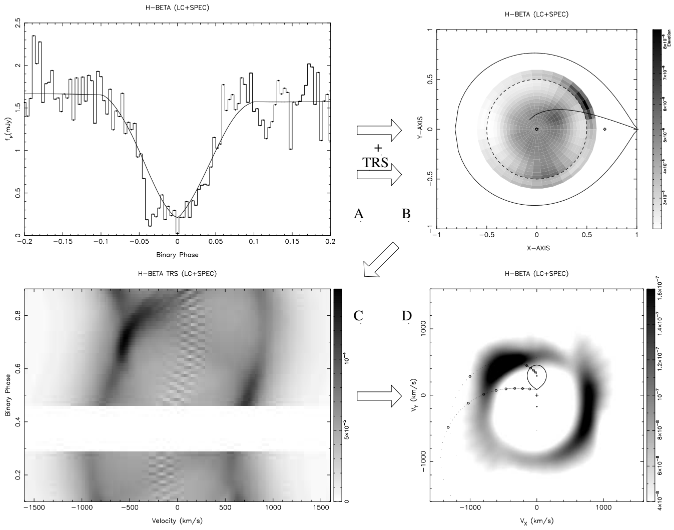

Fig. 8. Double dataset reconstruction in H_β, using the light curve and the trailed spectra shown in Fig. 6 top middle, as input dataset. Panel A in this plot shows the input data and the fit to the light curve (solid line). Panel B shows the reconstruction in position-coordinate representation. Panel C presents the trailed spectra, derived from the map in panel B under the assumption of a Keplerian velocity field. Panel D visualizes the corresponding Doppler-map in velocity-coordinates.

the rim, i.e. left and right of the primary, seen from the secondary. These artifacts would account for the orbital variations in the light curve and for the constant flux of light contributed by the secondary. This artifacts are the equivalent of the ring-like artifacts found by Rutten et al. (1992a) (1992b) which are arising from the uneclipsed light of the secondary. Because of our different reconstruction geometry, the effect of uneclipsed light is also different. But in the reconstructions we could not see any signature of the secondary in the position-coordinate representation.

Comparing the results in this paper with our results in Wolf et al. (1998), where we presented reconstructions using the same dataset, but using the light curve as only input dataset, the quality of the reconstruction has highly increased, and the intensity distribution is more reliable now. The original Doppler maps and the Doppler maps from the Double Dataset Reconstructions are very similar. The Doppler maps in Wolf et al. (1998) (Figs. 11, 12 and 13 therein), show a third accumulation of intensity around $(V_X, V_Y) = (-600, -400)\ km/s$. In contrast to the paper of Wolf et al. (1998) neither the orginal Doppler maps (Fig. 6) nor the Doppler maps derived from the Double Dataset reconstructions show such a third spot (Figs. 7, 8 and 9). So our Double Dataset reconstructions and the original data are consistent. The reconstructions in position-coordinate representation (panels B) have a better resolution in the Double Dataset Reconstructions. Also comparing the H_γ and H_β reconstructions with our results in Wolf et al. (1998) we can see that the central disc emission in the eclipse-maps is more consistent.

4. Discussion and Outlook

With simultaneously recorded spectroscopy and spectrophotometry, we are able to reconstruct accretion disks with the Double Dataset Eclipse Mapping method in emission lines. The reconstructions are reliable and free of artifacts. The application to observational data gives much better reconstructions compared with previous Single Dataset reconstructions where only the light curve was used as input dataset (Wolf et al. 1998). The reconstructed H_γ-, H_β- and H_α-eclipse-maps of the cataclysmic variable IP Peg, show a clear asymmetry. The inner regions of the disk are more prominent in the bluer wavelengths, the asymmetry in the redder ones. The asymmetry is located at the lower half of the maps in the reconstruction (approx. $(X; Y) = (0.0; -0,4)$ in Fig. 7, 8 and 9).

Makita et al. (1998) calculated two and three dimensional numerical simulations of accretion disks. They got spiral structures in the disk and a slight asymmetry, which is roughly comparable to our results. We could not definitely confirm a spiral structure during this state of quiescence from our reconstructions. Spiral structures in IP Peg during outburst were detected by Steeghs et al. (1997), and further analyzed by Steeghs & Stehle (1998). The simulations of Steeghs & Stehle (1998) show that strong spiral shocks can be formed in an accretion disk short before an outburst. They also calculated spiral shocks in an quiescent accretion disk and found out, that the spiral structures there are tightly wound in the inner regions of the disk and more wide in the outer disk. These spirals should be detectable as arcs in outer regions of the corresponding Doppler-map. Our re-analyzed datasets show in the eclipse-maps of H_γ and H_β

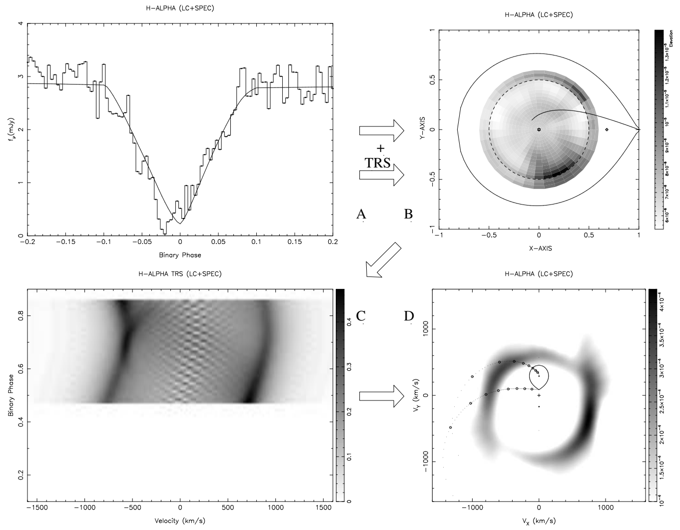

Fig. 9. Double dataset reconstruction in H_α, using the light curve and the trailed spectra shown in Fig. 6 top right, as input dataset. Panel A in this plot shows the input data and the fit to the light curve (solid line). Panel B shows the reconstruction in position-coordinate representation. Panel C presents the trailed spectra, derived from the map in panel B under the assumption of a Keplerian velocity field. Panel D visualizes the corresponding Doppler-map in velocity-coordinates.

an emission in the inner parts of the accretion disk, as well as emission from neighboring regions near the hot spot and outer disk regions opposite to the hot spot. These features are resolved in the Doppler maps as two contrary located arcs, one certainly belonging to the emission from the regions around the hot spot (Spruit & Rutten 1998), the other representing structures similar to a spiral structure simulated by Steeghs & Stehle. Since IP Peg was observed in an unusual strong outburst almost three weeks after our observation (Nogami 1995), we are not able to decide, if we can see in our reconstructions the beginning of the formation of a spiral or if the dataset is not sufficient enough to reconstruct a present spiral with the necessary clarity. Definitive answers for the nature and origin of spirals or asymmetric intensity distributions in accretion disks can only be given by simultaneous spectrophotometric and spectroscopic measurements at large telescopes, or with a further improved Eclipse Mapping Method (Bobinger, 1999, in prep.). With a better signal to noise ratio and better time resolution these observations would significantly improve the spatial resolution of the eclipse maps and therefore resolve the signatures of the interesting regions.

The Double Dataset Eclipse Mapping needs an assumed velocity field to mediate between position-coordinate representation and trailed spectra. From there the idea arises to use the Doppler maps derived from the original spectra as an additional dataset. This "Triple Dataset Eclipse Mapping" should be able not only to reconstruct the true intensity distribution but also the velocity-field.

Acknowledgments

The authors would like to say Thank You to all the helpful CV-people in our institute and at MPA and MPE Garching, especially to Alex Fiedler, Bernhard Deufel, Danny Steeghs, Sonja Vrielmann. in particular we would like to thank R. Hessmann for assistance during the observation run and to H.C. Thomas for his usefull remarkes on our work. A. Bobinger is very thankful to Prof. Keith Horne for many fruitful discussions, many inspirations, the "classical" eclipse mapping code and many other useful programs. Half an hour of discussion with him always inspired half a year of wonderful new science.

This work is supported by the Deutsche Forschungsgemeinschaft (grant Ma 1693/4-1).

References

Baptista R., Steiner J.E., 1993, A&A, 277, 331
Barwig H., Schoembs R., Buckenmayer C., 1987, A&A, 175, 327
Bobinger A., Horne K., Mantel K.H., Wolf S., 1997, A&A, 327, 1023
Horne K., 1985, MNRAS, 213, 129
Horne K., 1991, in: Fundamental Properties of Cataclysmic Variable Stars: 12th North American Workshop on Cataclysmic Variables and Low Mass X-ray Binaries. San Diego 3-5 Jan 1991., ed. Shafter, A.W., San Diego State University Publication, p. 23
Horne K., 1993, in: Accretion Disks in Compact Stellar Systems, ed. Wheeler J.C., World Scientific Publishing Company
Horne K., 1995, A&A, 297, 273
Horne K., Cook M.C., 1985, MNRAS, 216, 307
Horne K., Marsh T.R., 1986, MNRAS, 218, 761
Horne K., Marsh T.R., Chen, F.H., Hubeny I.L., 1994, ApJ, 426, 294
Lipovetskij V.A., Stephanyan J.A., 1981, Astrofisika, 17, 573
Makita M., Miyawaki K., Matsuda T., 1998, MNRAS, in press
Mantel K.H., Barwig H., 1993, NATO ASI series, C436,329
Mantel K.H., Barwig H., Kiesewetter S., 1993, "The MEKASPEK Project – a new step towards the utmost photometric accuracy", in: Proc. of the IAU Coll. 136, "Stellar Photometry", Dublin, edts. C.J. Butler, I. Elliot, Cambridge University Press, p. 172
Marsh T.R., 1988, MNRAS, 231, 1117
Marsh T.R., Horne K. 1988, MNRAS, 235, 269
Nogami D. 1995, In: Basic Physics of Accretion Discs, eds.: Kato S. et al. ., Gordon and Breach Science Publishers
Rutten R.G.M., 1998, A&AS127, 581
Rutten R.G.M., van Paradijs J., Tinbergen J., 1992a, A&A, 260, 213
Rutten R.G.M., Kuulkers E., Vogt N., van Paradijs J., 1992b, A&A, 265, 195
Rutten R.G.M., Dhillon V.S., 1994, MNRAS, 28, 773
Šimić D., Barwig H., Bobinger A., Mantel K.H., Wolf S., 1998, A&A, 329, 115
Skilling J., 1981, Workshop on Maximum Entropy Estimation and Data Analysis, University of Wyoming, Reidel, Dordrecht, Holland
Skilling J., Bryan R.K., 1984, MNRAS, 211, 111
Spruit H., Rutten R.G.M., 1998, MNRAS, in press
Steeghs D., Harlaftis E.T., Horne K., 1997, MNRAS, 290, L28
Steeghs D., Stehle R., 1998, MNRAS, in press
Wolf S., Barwig H., Bobinger A., Mantel K.H., Šimić D., 1998, A&A, 332, 984
Wood J.H., Horne K., Berriman G., Wade R.A., 1989, ApJ, 341, 974

This article was processed by the author using Springer-Verlag LaTeX A&A style file *L-AA* version 3.